Numerical Study on the Bearing Behaviour of Pile Groups Subjected to Lateral Pressure Due to Soil Movements

O. Reul[1], J. Bauer[2] and C. Niemann[3]
Department of Geotechnical Engineering, University of Kassel, Germany
E-mail: o.reul@uni-kassel.de

ABSTRACT: In soft soil layers vertical piles are frequently loaded laterally by horizontal soil movements caused by eccentric loading or unloading of the ground surface around the piles. In the course of the construction process of a steel mill a large scale test was carried out to investigate the influence of a storage for steel slabs on the pile foundation of a neighbouring bridge crane. In the scope of this paper the results of the measurements carried out during the large scale test are compared with three dimensional, coupled pore pressure-displacement finite element analyses investigating the influence of a thin stiff layer within a deposit of soft soil and the roughness of the pile-soil interface on the lateral pressure acting on the piles.

1. INTRODUCTION

In soft soil layers vertical piles are frequently loaded laterally by horizontal soil movements caused by eccentric loading or unloading of the ground surface around the piles (Figure 1). In many cases, the lateral pressure acting on piles due to horizontal soil movements is calculated with empirical formulae or analytically based on earth pressure theory, respectively. However, these calculation methods do not consider possible influences on the resulting pile loads such as the roughness of the pile-soil-interface, the pile geometry or the time dependent material behaviour of soft soil.

In the scope of this paper the results of a large scale test are subjected to a numerical back analysis investigating the influence of

- a thin stiff layer within a deposit of soft soil and
- the roughness of the pile-soil-interface on the lateral pressure acting on piles.

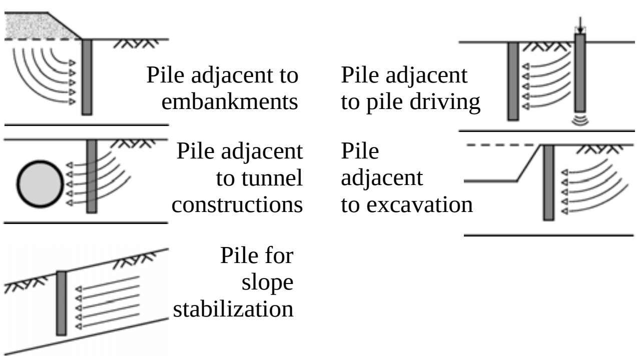

Figure 1 Lateral pressure on piles due to horizontal soil movement (after Chen 1994)

2. LARGE SCALE TEST

In the course of the construction process of a steel mill in Brazil (Glockner et al. 2008), a large scale test was carried out to investigate the influence of a storage for steel slabs (slab yard) on the pile foundation of a neighbouring bridge crane. The design of the pile foundation against lateral pressure was based on the measurements carried out during the large scale tests (Mühl et al. 2011) and the results of three dimensional, coupled pore pressure-displacement finite element analyses (Reul et al. 2013).

Originally, the site of the steel mill comprised swamp and grassland with its ground surface approximately 1 m above sea level. For the construction project the site has been filled up 1.5 m to 2 m with approximately $3.5 \cdot 10^6$ m³ of sand. The sand was dredged in the course of the construction works for a new deepwater port (Glockner et al. 2008). The groundwater level is situated on a level with the original ground surface. The subsoil at the site is characterised by deep fluviatile sediments. Beneath the sand fill alternating quaternary layers of very soft clays and sand are found. The up to 40 m thick quaternary is underlain by rock comprising mainly Gneiss and Granite, respectively. On its upper 1 m to 5 m the bedrock is weathered to various degrees. As an example, Figure 2 shows the results of a SP-test and a CPTU-test together with the corresponding soil profile.

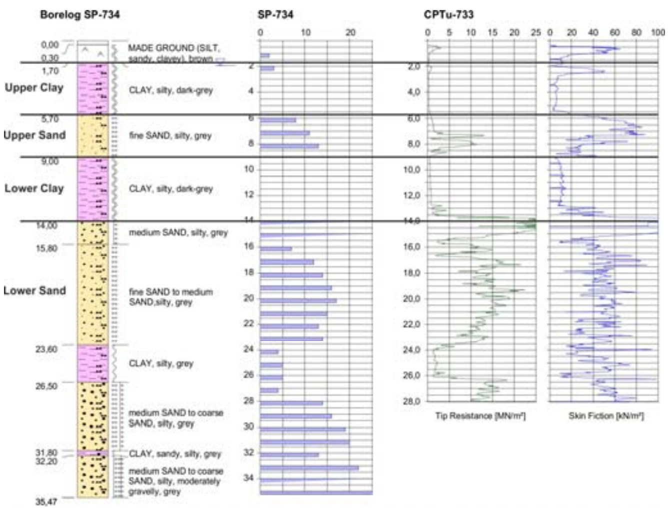

Figure 2 Soil profile in the area of the slab yard (Mühl et al. 2009)

The soil properties of the Upper and the Lower Clay are summarised in Table 1. The Upper Clay is a normally consolidated organic clay (Soil group OT according to DIN 18196) containing approximately 85 % fine particles (< 0.06 mm; clay particles approximately 36 %). Close to the ground surface the Upper Clay is slightly overconsolidated with undrained shear strength of up to c_u = 30 kN/m². Compared to the Upper Clay the Lower Clay (Soil group OT/TA or TM/TL, respectively, according to DIN 18196) shows lower liquidity indices and higher undrained shear strength with a content of 85 % fine particles (clay particles approximately 47 %). For both clay layers the liquidity indices generally were $I_L \geq 1$. However, it has to be noted that the Atterberg limits w_L and w_P are established using disturbed soil samples. For undisturbed conditions in-situ, a higher soil stiffness can be expected due to thixotropic soil behaviour (Schultze & Muhs 1967). Therefore the consistency of the clay layers can be described as mainly very soft (Upper Clay) or very soft to soft (Lower Clay), respectively.

The Upper Sand is loose to medium dense. In the medium dense to dense Lower Sand soft to stiff clay layers with a thickness of up to several meters are included. In a depth of approximately 34 m to

40 m the Lower Sand is underlain by weathered rock which can be classified as a gravelly, silty sand or sandy silt, respectively. The intact rock shows a mean unified compression strength of $q_u = 69$ MN/m^2.

Table 1 Properties (mean values) of the Upper and Lower Clay

Properties			**Upper Clay**	**Lower Clay**
Specific weight	γ	kN/m^3	13	14
Natural water content	w	%	113	73
Liquid limit	w_L	%	76	66
Plastic limit	w_P	%	44	35
Initial void ratio	e_0	-	2.9	2.2
Organic content	V_{gl}	%	6	n. s.
Compressibility index	C_c	-	0.5	0.3
Swelling index	C_s	-	0.04	0.04
Coefficient of secondary compression	C_α	-	0.03	0.01
Coefficient of vertical consolidation	c_v	m²/s	$8{\cdot}10^{-9}$	$9{\cdot}10^{-9}$
Undrained shear strength	c_u	kN/m²	16	45

It was the aim of the large scale test to optimize the design parameters for lateral pressure given by the German piling guideline "EA-Pfähle" (DGGT 2012), which had been applied for the pre-design (Mühl et al. 2009). A detailed description of the large scale test including a documentation of the test results is given by Mühl et al. (2011).

For the large scale test, two concrete foundations with dimensions of 7.0 m × 4.0 m × 2.2 m have been founded on four and five driven steel piles (Diameter d_p = 813 mm, wall thickness t = 15 mm, pile base 35 m to 40 m below ground level), respectively. Additionally two comparable single piles have been installed. The piles embedded in the intact rock showed an ultimate vertical capacity of $R_{1,k}$ = 7 MN derived from dynamic pile tests (wave matching analysis of dynamic signals). Between the two foundations a reinforced concrete raft (Area size A = 33 m × 40 m; raft thickness t_r = 0.6 m) was placed to distribute the load of the steel slabs and to prevent local base failure mechanisms. Beneath the raft and the foundations geosynthetic vertical drains have been installed to accelerate the consolidation process. After the test the two pile foundations have been used for the actual crane bridge.

The instrumentation of the large scale test is shown in Figure 3 and Figure 4. Amongst others, the following parameters have been measured:

- Pore pressures in the clay layers.
- Earth pressures in the clay layers.
- Horizontal displacements of the soil.
- Settlements and deflection of the raft.
- Horizontal displacements of the foundations.
- Horizontal displacements and stresses in the piles.

For the loading of the raft iron ore with a specific weight of γ = 27 kN/m³ to γ = 35 kN/m³ was applied. At the edge of the raft the embankment was supported by a retaining wall made of so called BigBags filled with iron ore. The loading sequence followed the primarily intended stock keeping concept during the starting phase of the steel slab production (Mühl et al. 2009).

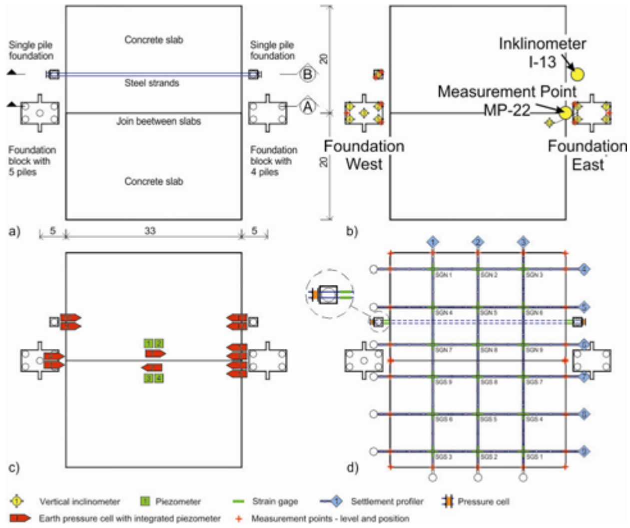

Figure 3 Large scale test: Ground plan (Mühl et al. 2011)

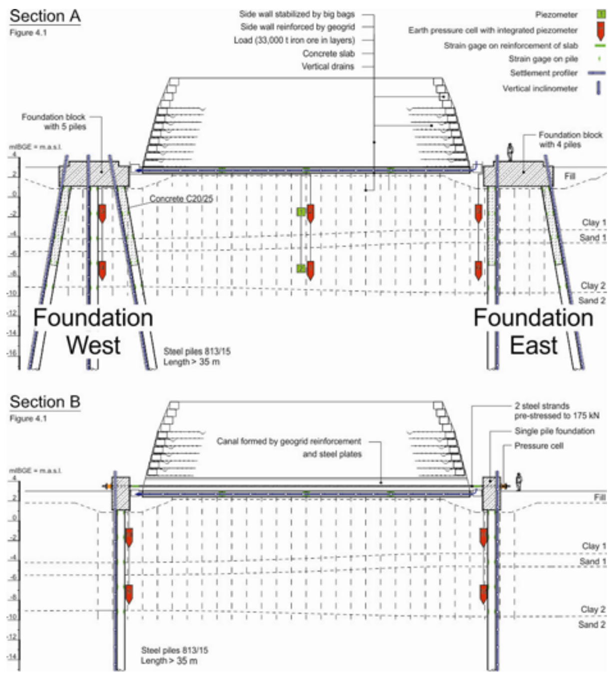

Figure 4 Large scale test: Cross section (Mühl et al. 2011)

3. NUMERICAL MODEL

3.1 Geometry

The numerical study was carried out by means of three dimensional finite element analyses. With the coupled pore pressure-displacement analyses the time dependent displacement caused by consolidation processes as well as by the material behaviour of the soft clayey soils is modelled. The finite element mesh comprises approximately 41,000 hexahedral elements with both displacements and pore pressures varying linearly across the elements. All analyses presented in the scope of this paper are based on small strain theory.

Figure shows the finite element mesh. In the model the following geometrical constraints have been considered:

- Ground surface: 3.3 msl (3.3 m above sea level)
- Groundwater level: 3.3 msl
- Foundation level: 1.1 msl
- Pile base: -33.8 msl

Only the soil below the foundation level is modelled with finite elements. The soil above the foundation level is considered through its weight.

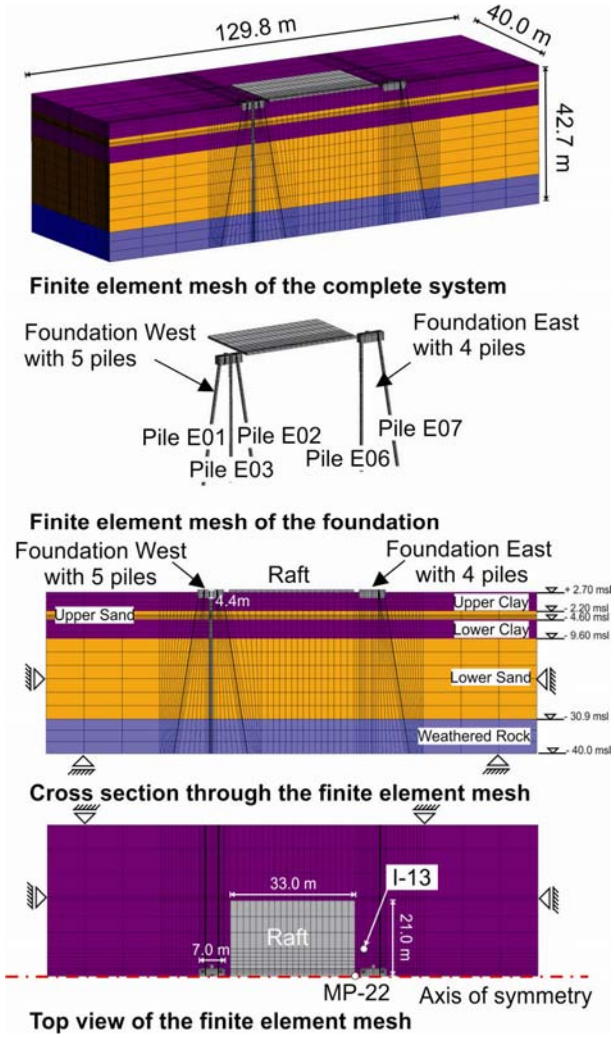

Figure 5 Finite Element Mesh

The thickness of the Upper Sand varies significantly in the test area between approximately 0.5 m and 3.3 m. Compared to the design analyses where the Upper Sand has been modelled with a thickness of 1.3 m (Reul et al. 2013), in the scope of the analyses presented in this paper a thickness of 2.4 m has been adopted to achieve a better agreement with the measurements.

In the finite element model the circular piles have been replaced by octagonal piles with approximately the same shaft circumference c_s (Figure 6). Up to a depth of -6.5 msl a composite section comprising a steel tube with a concrete filling has been considered. Below this depth only the stiffness of the steel tube has been modeled.

Instead of modelling the vertical drains directly in the finite element analyses, appropriately enhanced consolidation parameters have been adopted (Section **Error! Reference source not found.**). Based on the measurements and the results of the calibration analysis it was concluded that the drains in the Lower Clay are not effective (Section 4.1).

3.2 Material behaviour

The material parameters applied for the clay and sand layers and for the underlying rock are the results of a calibration analysis based on the measurements of the large scale test.

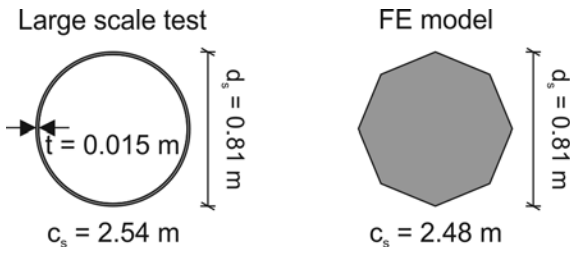

Figure 6 Finite Element mesh: Detail of the investigated pile cross section

The material behaviour of the sand layers and the underlying rock has been modeled with a linear elastic-perfect plastic soil model applying the Mohr-Coulomb failure criteria defined by the shear parameters c‘ and φ‘. For the plastic deformations constant volume was assumed, i. e. a nonassociated flow rule has been applied.

The material behaviour of the clay layers has been modeled with the visco-hypoplastic soil model by Niemunis (1996, 2003). A short description of the soil model which has been extended to incorporate intergranular strains (Niemunis & Herle 1997) is given in FEAT (2013). The verification of the visco-hypoplastic soil model was carried out by means of the back-analysis of a representative oedometric test on a sample taken from the Upper Clay. Punlor (2004) gives an instruction how to derive the parameters of the visco-hypoplastic soil model from lab tests. The parameters applied in the scope of this paper are based on lab tests carried out in the scope of the site investigation, on data published on clayey soils (Krieg 2000, Punlor 2004, Garcia et al. 2006, Lizcano et al. 2007, Meier 2009) and on the calibration analyses taking the available measurements into account. Based on the results of dilatometer tests, lab tests and the earth pressure measurements during the large scale test, Thá et al. (2010) suggest earth pressures at rest of K_0 = 0.9 (Upper Clay) and K_0 = 0.8 (Lower Clay), respectively. Under consideration of the following approach documented for example by Niemunis (1996)

$$K_0 = \frac{a}{a+3} \tag{1}$$

with

$$a = \frac{\sqrt{3}\cdot(3-\sin\varphi_c)}{2\cdot\sqrt{2}\cdot\sin\varphi_c} \tag{2}$$

an earth pressure at rest of K_0 = 0.555 has been applied for the Upper Clay and the Lower Clay.

Interface elements with a linear elastic-perfect plastic material behaviour have been applied for the simulation of the pile-soil-interaction. For the applied Mohr-Coulumb failure criteria the shear parameters of the surrounding soil have been used. If not indicated otherwise all results presented in the scope of this paper have been derived for a interface shear strength ratio R_{inter} = 1.0. The interface shear strength ratio R_{inter} is defined as

$$R_{inter} = \frac{tan\,\varphi_i}{tan\,\varphi_{soil}} = \frac{c_i}{c_{soil}} \tag{3}$$

with φ_{soil} = friction angle of soil, φ_i = friction angle of interface, c_{soil} = cohesion of soil and c_i = cohesion of interface. For the normal and tangent stiffness of the interface Young’s modulus and shear modulus of the pile, respectively, have been adopted to model almost rigid-plastic interface behaviour as suggested for example by Cai & Ugai (2000). A discussion of the influence of the contact model between pile and soil on the lateral pressure acting on piles can be found for example in Aschrafi et al. (2013).

The raft, the foundations and the piles are considered to behave linear-elastically. The stiffness of the piles has been modelled by means of an equivalent Young's modulus E*. With the equivalent Young's modulus E* the bending stiffness E*·I of the octagonal piles in the finite element model is the same as the bending stiffness of the composite section $(E \cdot I)_{composite}$ or the bending stiffness of the hollow steel tube $(E \cdot I)_{steel\ tube}$, respectively.

The permeability of the clay is assumed to be isotropic and a function of the void ratio (Figure 7).

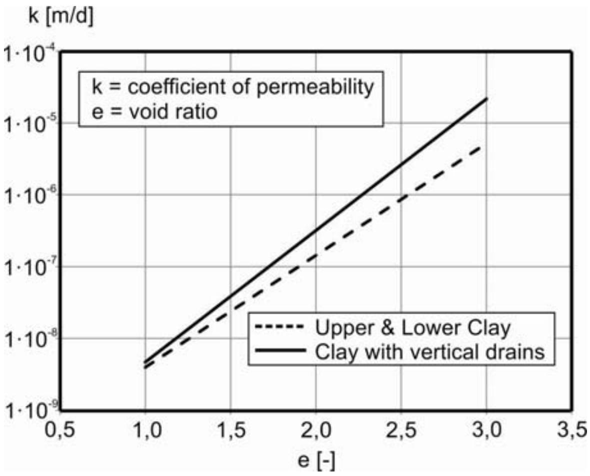

Figure 7 Permeability of the clay depending on the void ratio

The material parameters applied in the finite element analyses are summarized in Table 2, Table 3 and Table 4.

Table 2 Material properties of the clay

Properties			**Upper Clay**	**Lower Clay**
Specific weight	γ	kN/m³	14	
Buoyant unit weight	γ'	kN/m³	6	
Residual friction angle	φ_c	°	25	
Poisson's ratio	ν	-	0.25	
Reference creep rate	D_r	1/s	$1 \cdot 10^{-6}$	
Viscosity index	I_v	-	0.04	
Void ratio for reference stress (p_{e0} = 56 kN/m²)	e_{e0}	-	2.339	
Coefficient of earth pressure at rest	K_0	-	0.555	
Intergranular strain	R; m_R; m_T; β_χ; χ	-	$1 \cdot 10^{-4}$; 4.5; 4.5; 0.3; 8.0	
Slope of the first compression line	λ	-	0.0700	0.0650
Slope of the swelling/reloading line	κ	-	0.0125	0.0120
Shape parameter	β_R	-	0.95	
Coefficient of permeability	k	m/d	Figure	

Table 3 Material properties of the sand and the rock

Properties			**Upper Sand**	**Lower Sand**	**Rock**
Specific weight	γ	kN/m³	19	19	19
Buoyant unit weight	γ'	kN/m³	10	10	10
Young's modulus	E	MN/m²	50	200	600
Poisson's ratio	ν	-	0.25	0.25	0.25
Cohesion	c'	kN/m²	0	0	50
Friction angle	φ'	°	32.5	32.5	32.5
Angle of dilatancy	ψ	°	0	0	0
Coefficient of earth pressure at rest	K_0	-	0.46	0.46	0.46
Coefficient of permeability	k	m/d	$7.2 \cdot 10^{-4}$ *1 / $3.6 \cdot 10^{-3}$ *2	$3.6 \cdot 10^{-2}$	$3.6 \cdot 10^{-1}$

*1 Sand without Drains
*2 Sand with Drains

Table 4 Material properties of piles, pile head foundation and raft

Properties			Piles	Pile head foundations & raft
Specific weight	γ	kN/m³	-	25
Buoyant unit weight	γ'	kN/m³	15	-
Young's modulus	E	MN/m²	84600*1 / 45000*2	30000
Poisson's ratio	ν	-	0.2	0.2

*1 Equivalent Young's modulus of the hollow steel tube filling with concrete $(E \cdot I)_{composite}$
*2 Equivalent Young's modulus of the hollow steel tube $(E \cdot I)_{steel\ tube}$

3.3 Step-by-step analysis of the loading process

In the finite element analysis the loading scheme of the large scale test was applied in a step-by-step-analysis. The piles have been "wished-in-place", i.e. pile driving, displacement of soil and changes in the soil surrounding the pile caused by the installation process have not been modelled.

Similarly, the effects of the installation of the vertical drains on the surrounding soil have not been modelled. This is obviously a simplification since the installation disturbance affects the vertical and the horizontal coefficients of permeability (Bergado et al. 1991) as well as the strength properties of the soil in the smear zone surrounding a vertical drain.

The loads steps in the finite element analysis are summarized in Table 5.

4. RESULTS

4.1 Comparison of measurements and finite element analysis

Figure 8 shows the variation of the settlements of the northern section of the raft with time. The measurement points are situated only at the edge of the raft (Figure 3) and therefore measurements at the centre of the raft where the settlements would be expected to be largest are not available. The construction of the raft on 16.09.2008 was defined as the start of the test. Since the initial measurement was carried out on 02.10.2008 the immediate settlement due to the weight of the raft as well as a fraction of the consolidation- and creep-settlements are not included in the following evaluation. For a better overview only the measurement point MP22 with the largest measured settlements after the final load step are presented. The position of the measurement point is shown in the finite element mesh in Figure 5. It has to be noted that for the calibration of the soil model the maximum measured settlements have been taken as reference values.

Table 5 Step-by-step analysis of the loading process

Calculation step		Start [d]	Duration of installation/ of load step [d]	Load on raft q [kN/m²]
I	Initial stress state	-	-	-
II	Installation of piles	0	-	-
III	Installation of raft	0	1	-
IV	Load step 1	11	28	59
V	Installation of foundations	59	-	
VI	Load step 2	64	9	107
VII	Load step 3	120	10	154
VIII	Load step 4	175	11	202
IX	Load step 5	240	5	256
X	Unloading	339	14	0
XI	-	353	22	0

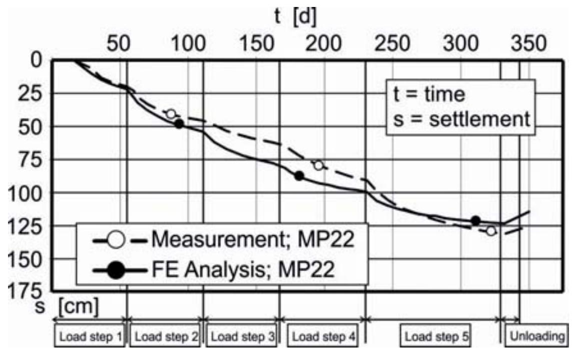

Figure 8 Variation of the raft settlements with time

Figure 9 compares the measured and calculated variation of the excess pore pressures with time at the pore pressure cells in the Upper Clay (PZ 1-1 & PZ 1-3) and the Lower Clay (PZ 1-2 & PZ 1-4) showing a reasonable agreement. However, especially in load step 5 the measured reduction of excess pore pressure proceeds slower than in the finite element analysis. This indicates probably a stronger influence of the void ratio on the permeability than has been taken into account in the model (Figure 7). Another reason could be a degradation of the performance of the vertical drains. Based on the observation that the excess pore pressures in the Lower Clay (PZ 1-2 & PZ 1-4) are significantly higher than in the Upper Clay (PZ 1-1 & PZ 1-3) it was concluded that the drains in the Lower Clay are not effective.

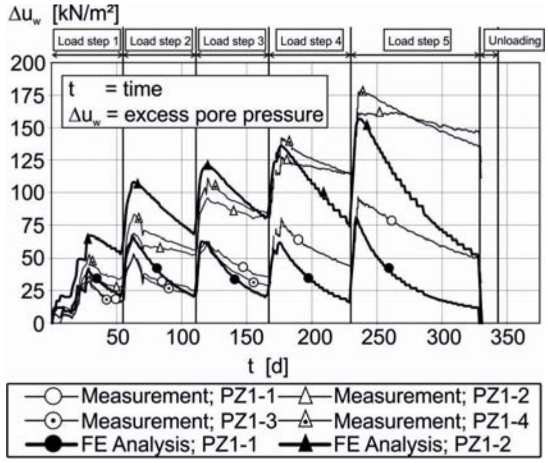

Figure 9 Variation of excess pore pressures with time

Measurements and finite element analysis show the Mandel-Cryer-effect (e.g. Schiffman et al. 1969) which has previously been observed for example in numerical simulations of foundations such as piled rafts (Cui et al. 2009) or skirted foundations (Gourvenec & Randolph 2010). The Mandel-Cryer-effect is a characteristic effect of three-dimensional consolidation with the excess pore pressure increasing over the initial increase in total stress due to the externally applied load. In load step 5 for example, the excess pore pressure at PZ1-2 amounts to Δu_{FE} = 81 kN/m² and $\Delta u_{Measurement}$ = 65 kN/m², respectively, while the externally applied load increment is only Δq = 54 kN/m².

The measured and calculated horizontal displacements of piles E01, E02 and E03 (Foundation West) and piles E06 and E07 (Foundation East) are shown in Figure 10 for 22.07.2009, i.e. during load step 5. The horizontal displacements calculated in the finite element analysis have been related to the 31.10.2008 which is the date of the initial measurement of the inclinometer. While there is a reasonable agreement between measurement and analysis for the piles of Foundation West (E01, E02 and E03) the horizontal displacements for the piles of Foundation East (E06 and E07) are significantly overestimated in the finite element analysis. Similarly, the calculated horizontal displacements at inclinometer I-13 located close to Foundation East (Figure 3) are considerably larger than the measured values Figure 11.

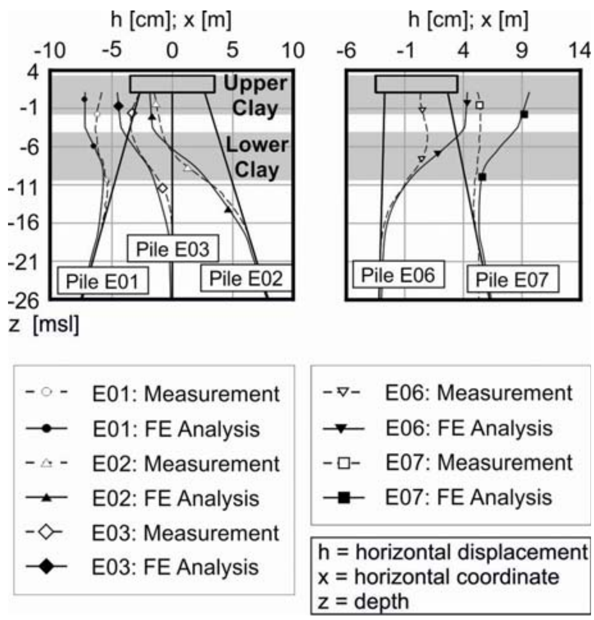

Figure 10 Horizontal displacements of the piles in load step 5

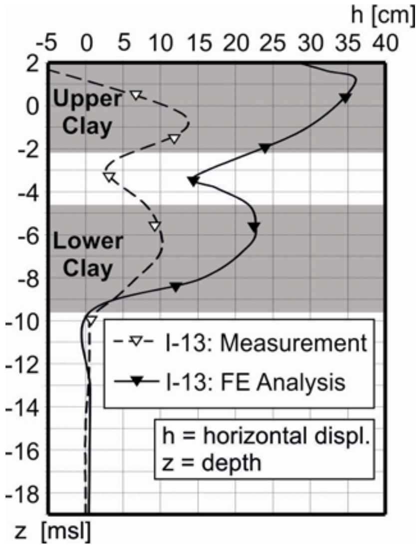

Figure 11 Horizontal displacements of inclinometer I-13 in load step 5

With the applied soil model it is possible to simulate the measured bearing behaviour of the foundation at least qualitatively. However, the deformations, especially the horizontal displacements of the piles under Foundation East, are overestimated in the finite element analysis

The following points possibly are responsible for the discrepancy between measurements and finite element analysis:

- The clay shows an anisotropic material behaviour with the horizontal stiffness being significantly larger than the vertical stiffness (Graham & Houlsby 1983). So far, this anisotropy is not incorporated in the applied visco-hypoplastic soil model.
- The thickness of the Upper Clay and the Lower Clay is very heterogeneous on the construction site. Therefore the mean thickness of the two clay layers in the vicinity of Inclinometer I-13 and Foundation East might be significantly smaller than modelled in the finite element analysis.

4.2 Lateral pressure

The estimation of lateral pressures based on earth pressure measurements yielded no plausible results and was not pursued (Mühl et al. 2011). In the scope of this paper therefore only lateral pressure established in the finite element analyses is presented. The lateral pressure p acting on the pile was derived from the normal stresses σ and shear stresses τ at the pile-soil interface as indicated in Figure 12. The evaluation of the distribution of normal stresses gave no indication for the development of a gap between pile and soil at the pile back, i.e. a normal contact pressure of $\sigma > 0$ was observed for all analysis steps.

Figure 13 shows the distribution of the lateral pressure along the pile shaft of pile E06 (Foundation East) for load step 5 (q = 256 kN/m²) with mean values of $p_{uc,m}$ = 141 kN/m (Upper Clay), $p_{us,m}$ = 483 kN/m (Upper Sand) and $p_{lc,m}$ = 179 kN/m (Lower Clay) for the different soil layers. The occurrence of the maximum lateral pressure in the Upper Sand will be investigated further in the next section.

4.3 Influence of the stiffness of the Upper Sand on the lateral pressure

To investigate the influence of stiff soil layers within a deposit of soft soil further, Young's modulus of the Upper Sand has been reduced from its initial value E = 50 MN/m² to E = 24.3 MN/m² and E = 1.4 MN/m², respectively. The latter value approximately corresponds to the mean Young's modulus of the Upper Clay for the in-situ stress level.

Figure shows the distribution of the lateral pressure along the pile shaft in the Upper Sand with the mean lateral pressure reducing from $p_{us,m}$ = 483 kN/m (E = 50 MN/m²) to $p_{us,m}$ = 289 kN/m (E = 1.4 MN/m²). The results imply that a thin stiff layer within a deposit of soft soil is swept away by the moving soft soil and pushed against the pile, yielding an increase of the lateral pressure with increasing layer stiffness. For a given horizontal displacement a stiff soil layer will apply a larger lateral pressure on the pile than a soft soil layer.

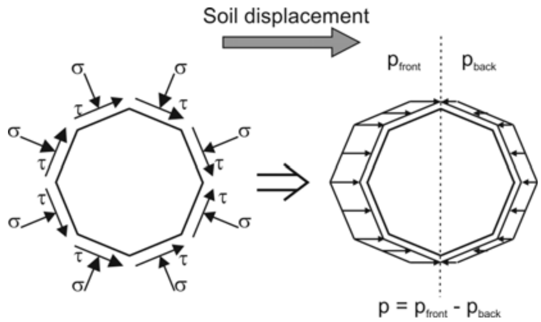

Figure 12 Lateral pressure acting on the pile derived from normal stresses and shear stresses at the pile-soil interface

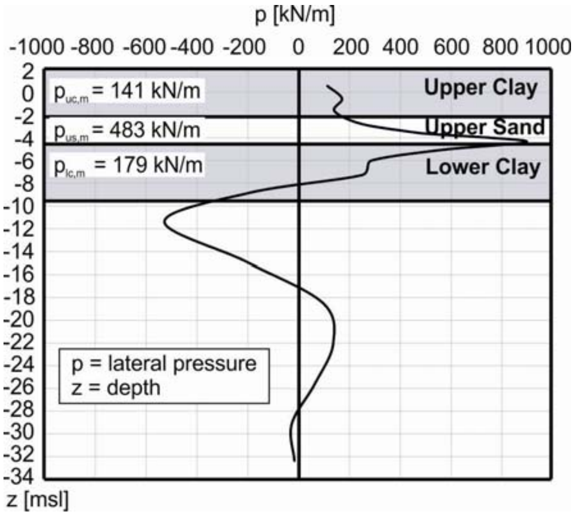

Figure 13 Distribution of the lateral pressure along the pile shaft for pile E06 in load step 5

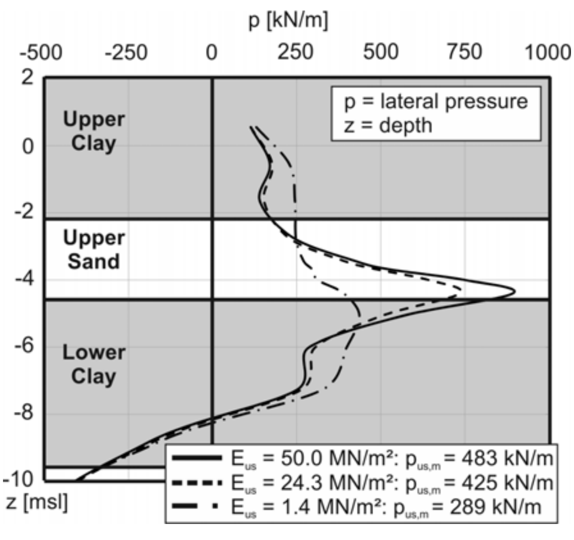

Figure 14 Distribution of the lateral pressure along the pile shaft of pile E06 for different stiffness of the Upper Sand

4.4 Influence of the interface shear strength on the lateral pressure

To investigate the influence of the pile roughness, on the analysis, the interface shear strength ratio R_{inter} (Eq. (3)) has been varied between $R_{inter} = 0.33$ and $R_{inter} = 1.00$ simultaneously for all four soil layers. Figure 15 shows the variation of the calculated lateral pressure with the interface shear strength ratio for the load steps 2 (q = 107 kN/m²) and 5 (q = 256 kN/m²). Load step 2 and 5 correspond with horizontal displacements of pile E06 of $h/d_s = 0.02$ (load step 2) and $h/d_s = 0.09$ (load step 5), respectively, in the Upper Clay and $h/d_s = 0.01$ (load step 2) and $h/d_s = 0.06$ (load step 5), respectively, in the Lower Clay. For load step 2 only the lateral pressure in the Lower Clay increases with increasing interface shear strength ratio by 4 %. For load step 5 an increase of the lateral pressure can be observed in the Lower Clay (4 %) and in the Upper Sand (2 %). In the Upper Clay however, the lateral pressure even decreases slightly by 2 %.

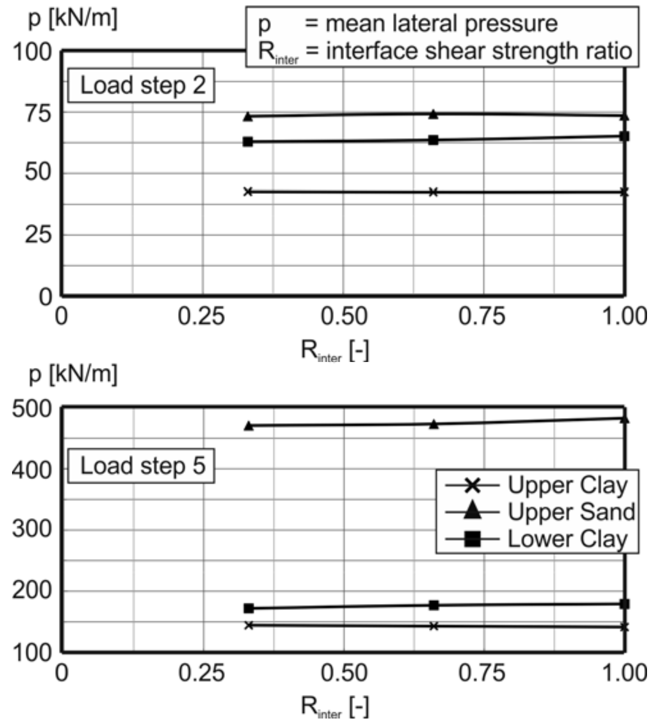

Figure 15 Variation of the lateral pressure with the interface shear strength ratio (pile E06; load steps 2 & 5)

These results show a significantly less pronounced influence of the interface shear strength ratio, i. e. the pile roughness, than established theoretically and from experimental studies. Based on plasticity theory Randolph & Houlsby (1984) predict an increase of lateral pressure between perfectly smooth and rough piles of approximately 31 % for homogeneous soft soils. In small scale model test in normally consolidated kaolin clay Bauer et al. (2014) measured an increase of lateral pressure between smooth (plain aluminium profiles) and rough (sandpaper glued of the aluminium profiles) piles between 19 % and 32 %, depending also on the undrained shear strength of the soil. So far, it is assumed that the following aspects mainly contribute to the only small influence of the interface shear strength ratio on the lateral pressure observed in the current analyses:

- The horizontal displacements of the piles presented in the scope of this paper are relatively moderate. Larger horizontal displacements will result in increased lateral pressures and due to the increased relative displacements between pile and soil probably in an increased influence of the pile roughness.
- The foundation at the pile head prevents a free soil movement at least at the top of the Upper Clay.
- The relatively stiff Upper Sand dominates the development and distribution of lateral pressure on the pile, making the comparison of the results with solutions for homogenous soft soil layers difficult.

5. COMPARISON OF ANALYSIS RESULS WITH COMMON DESIGN APPROACHES FOR THE LATERAL PRESSURE

According to Poulos (1989) and Stewart et al. (1994) the broad groupings for existing design methods are empirical methods, pressure-based methods, displacement-based methods and finite element analyses. However, design methods where the lateral pressure is calculated based on the undrained shear strength of the soil, the pile diameter or pile edge length, respectively, and an empirically or theoretically motivated correlation factor prevail.

According to EA-Pfähle (DGGT 2012) the decisive characteristic lateral pressure p_k can be estimated with the following approach:

$$p_{f,k} = 7 \cdot \eta_a \cdot c_{u,k} \cdot D_s \tag{4}$$

$$p_{e,k} = b \cdot \Delta e_k = b \cdot \left(e_{a,k} - e_{p,k}\right) \tag{5}$$

$$p_k = Minimum \begin{Bmatrix} p_{f,k} \\ p_{e,k} \end{Bmatrix} \tag{6}$$

with $p_{f,k}$ = lateral pressure, $c_{u,k}$ = undrained shear strength, D_s = pile diameter, η_a = coefficient according to Wenz (1963), $p_{e,k}$ = lateral pressure calculated under consideration of the resulting earth pressure, $e_{a,k}$ = active earth pressure, $e_{p,k}$ = passive earth pressure, b = width of influence and L_p = pile length subjected to lateral pressure.

Consecutively, for the two pile groups East and West the lateral pressure is estimated with the approach given in EA-Pfähle (DGGT 2012) for load step 5 (q = 256 kN/m²). The undrained shear strength is assumed to be constant over the thickness of the clay layers with the mean values taken from Table 1. The subsoil profile corresponds to the finite element model. The active earth pressure $e_{a,k}$ as well as the passive earth pressure $e_{p,k}$ are calculated for undrained conditions with the approach given by the EA-Pfähle (DGGT 2012). Following this proceeding, the earth pressure yields the decisive value for the lateral pressure for the Upper Clay and the Lower Clay. The lateral pressure estimated with the approach given by EA-Pfähle (DGGT 2012) acting on the two pile groups East and West is summarized in Table 6.

Table 6 Decisive lateral pressure in the Upper and Lower Clay estimated with the approach given by EA-Pfähle (DGGT 2012)

	Pile group West			**Pile group East**	
	E01 [kN/m]	**E03 [kN/m]**	**E02 [kN/m]**	**E06 [kN/m]**	**E07 [kN/m]**
Upper Clay	151	173	216	243	189
Lower Clay	112	128	160	180	140
Coefficient k*	0.4	0.6	1.0	0.8	0.4

* Distribution of the lateral pressure according to Horch (1980) The lateral pressure has a constant value over the corresponding thickness of the soil layer.

Table 7 compares the lateral pressure in the Upper and Lower Clay estimated from various published approaches with the lateral pressure derived from the finite element analysis (Figure 13). To ensure comparability a coefficient of η_a = 1.55 as well as a pile diameter/edge length of $D_s = a_s$ = 0.81 m has been considered for all approaches. The lateral pressure derived from the finite element analysis lies within the bandwidth of these approaches. However, it has to be noted that the stiff Upper Sand plays a significant role in the development of lateral pressure in the over- and underlying layers, which is not considered in these approaches.

Table 7 Lateral pressure in the Upper and Lower Clay acting on pile E06

Approach		**p_k; $p_{f,k}$; $p_{e,k}$ [kN/m]**	
		Upper Clay	**Lower Clay**
Decisive lateral pressure estimated with the approach given by EA-Pfähle (DGGT 2012)	p_k	243	180
Finite element analysis (Figure)	p	141	179
EA-Pfähle (DGGT 2012)	$p_{f,k} = 7 \cdot c_u \cdot D_s$	141	395
Brinch Hansen/Lundgren (1960)	$p_{f,k} = 6.4 \cdot c_u \cdot D_s$	129	362
Schenk/Smoltczyk (1966)	$p_{f,k} = 2.6 \cdot c_u \cdot D_s$	52	147
Wenz (1972)	$p_{f,k} = 11.42 \cdot c_u \cdot a_s$	229	645
Fedders (1978)	$p_{f,k} = 10 \cdot c_u \cdot D_s$	201	565
Gudehus/Leinenkugel (1978)	$p_{f,k} = 4.5 \cdot c_u \cdot D_s$	90	254
Randolph/Houlsby (1984)	$p_{f,k} = 9.14 \cdot c_u \cdot D_s$	184	516
Pan et al. (2000)	$p_{f,k} = 10.6 \cdot c_u \cdot a_s$	213	599
Miao et al. (2006)	$p_{f,k} = 10.5 \cdot c_u \cdot a_s$	211	593

6. CONCLUSIONS

A reasonable qualitative agreement between the measured bearing behaviour of the pile foundation subjected to lateral pressure and the finite element analysis was achieved. Especially the consolidation process and the creep deformations have been reproduced well in the finite element analysis. One reason for the overestimation of horizontal displacements in the finite element analysis could be the possible anisotropy of the clay with a significantly higher horizontal stiffness. Anisotropy has not been considered in the applied visco-hypoplastic soil model and should therefore be implemented for future investigations.

In the presented analyses the stiff Upper Sand layer within the soft Upper and Lower Clay has a significant impact on the lateral pressure and especially the influence of the assumed sand layer thickness needs to be investigated further. Future research should also focus on the influence of the pile roughness and relative pile-soil displacement on the development of the lateral pressure.

The comparison of various approaches for the estimation of the lateral pressure acting on pile groups shows a large deviation of results. Therefore further investigations, especially on the influence of the following parameters should be carried out:

- geometry of pile and pile group,
- distance between surface loads and pile group,
- long term deformations
- soil strength,
- stress level in the soil.

7. REFERENCES

Aschrafi, J., Mühl, A., Glockner, A., Moormann, C. (2013) "Numerische Untersuchungen zur passiven Horizontalbeanspruchung von Pfählen in weichen bindigen Böden", Pfahl-Symposium 2013, Mitteilungen des Institutes für Grundbau und Bodenmechanik der TU Braunschweig, Heft 96, pp .283-302.

Bauer, J., Kempfert, H.-G., Reul, O. (2014) "Lateral pressure on piles due to horizontal soil movement - 1g model tests on single piles and pile rows", Proc. 8th International Conference on Physical Modelling in Geotechnics.

Bergado, D. T., Akasami, H., Alfaro, M. C., Balasubramaniam, A., S. (1991). “Smear effects of vertical drains on soft Bangkok clay”, ASCE, Journal of Geotechnical Engineering, Vol. 117, No. 10, pp. 1509-1530.

Brinch Hansen, J., Lundgren, H. (1960) "Hauptprobleme der Bodenmechanik", Springer-Verlag, Berlin, Göttingen, Heidelberg, pp. 266-268.

Cai, F., Ugai, K. (2000) "Numerical analysis of the stability of a slope reinforced with piles", Soils and Foundations, Vol. 40, No. 1, pp. 73-84.

Chen, L. T. (1994) "The effect of lateral soil movements on pile foundation", PhD thesis, University of Sydney, Australia.

Cui, C., Luan, M., Zhao, Y.(2009) "Time-dependent behavior of piled-raft on soil foundation with reference to creep and consolidation", Electronic Journal of Geotechnical Engineering (EJGE), Vol. 14A

Deutsche Gesellschaft für Geotechnik (DGGT), AK 2.1 (2012) "Empfehlungen des Arbeitskreises Pfähle – EA Pfähle", 2. Auflage, Ernst & Sohn,.

FEAT (2013) "Tochnog Professional" , Version 15.

Fedders, H. (1978) "Seitendruck auf Pfähle durch Bewegung von weichen bindigen Böden – Empfehlung für Entwurf und Bemessung", Geotechnik, 2, pp. 100-104.

Garcia, F., Lizcano, A., Reul, O. (2006) "Numerical modelling of the case history of a piled raft with a viscohypoplastic model", Proc. Numerical Modelling of Construction Processes in Geotechnical Engineering for Urban Environment, Bochum, Taylor & Francis Group, London, pp. 265-271.

Glockner, A., Moormann, C., Jud, H., Lindner, K.-J., Kunzmann, M., (2008) "Bau eines neuen Stahlwerks auf weichen Sedimentböden nahe Rio de Janeiro - Geotechnische Herausforderungen in ungewöhnlichen Dimensionen", Vorträge der Baugrundtagung 2008, Dortmund, DGGT, Essen, pp. 199-206.

Gouvernec, S., Randolph, M.F. (2010) "Consolidation beneath circular skirted foundations", International Journal of Geomechanics, Vol. 10, No. 1, pp. 22-29.

Graham, J., Houlsby, G.T. (1983) "Anisotropic elasticity of a natural clay", Géotechnique 33, No. 2, pp. 165-180.

Gudehus, G., Leinenkugel, H-J. (1978) "Fließdruck und Fließbewegung in bindigen Boden: Neue Methoden", Vorträge der Baugrundtagung 1978, Berlin, Deutsche Gesellschaft für Erd- und Grundbau, Essen, pp. 411-429.

Horch, M. (1980) "Zuschrift zu: Seitendruck auf Pfähle durch Bewegung von weichen bindigen Böden – Empfehlung für Entwurf und Bemessung", Geotechnik, 4, pp. 207-208.

Krieg, S. (2000) "Viskoses Bodenverhalten von Mudden, Seeton und Klei", Mitteilungen des Institutes für Bodenmechanik und Felsmechanik der TU Karlsruhe, Heft 150.

Lizcano, A., Rinaldi, V., Fuentes, W. M. (2007) "Visco-hypoplastic model for Pampean Loess", Mecánica Computacional, 26, pp. 2646-2655.

Meier, T. (2009) "Application of hypoplastic and viscohypoplastic constitutive models for geotechnical problems", Mitteilungen des Institutes für Bodenmechanik und Felsmechanik der TU Karlsruhe, Heft 171.

Miao, L. F., Goh, A. T. C., Wong, K. S., Teh, C. I. (2006) "Three-dimensional finite element analyses of passive pile behaviour", Int. Journal for Numerical and Analytical Methods in Geomechanics, 30, pp. 599-613.

Mühl, A., Röder, K., Glockner, A. (2009) "Untersuchung zum Seitendruck auf Pfähle einer Brückenkrananlage", Tagungsband 5. Freiberger Geotechnik Kolloquium, Freiberg, pp. 297-312.

Mühl, A., Thá, P. C., Glockner, A., Röder, K. (2011) "Instrumentation and Monitoring of a Full-Scale Test on Pile Foundations for Overhead Bridge Cranes", Proc. 8th International Symposium on Field Measurements in Geomechanics, Berlin.

Niemunis, A. (1996) "A visco-plastic model for clay and its FE-implementation", Resultants recents en mechanique des sols et des roches, Politechnika Gdanska, pp. 151-162.

Niemunis, A. (2003) "Extended hypoplasticity models for soils", Schriftenreihe des Instituts für Grundbau und Bodenmechanik der Ruhr-Universität Bochum, Heft 34.

Niemunis, A., Herle, I. (1997) "Hypoplastic model for cohesionless soils with elastic strain range", Journal of Mechanics of Cohesive-Frictional Materials, 4, Issue 2, pp. 279-299.

Pan, J. L., Goh, A. T. C., Wong, K. S., Teh, D. I. (2000) "Model tests on single piles in soft clay", Canadian Geotechnical Journal, 37, pp. 890-897.

Poulos, H. G. (1989) "Pile behaviour – theory and application", Géotechnique, 39, Issue 3, pp. 365-415.

Punlor, A. (2004) "Numerical modelling of the visco-plastic behaviour of soft soils", Mitteilungen des Institutes für Bodenmechanik und Felsmechanik der TU Karlsruhe, Heft 163.

Randolph, M. F., Houlsby, G. T. (1984) "The limiting pressure on a circular pile loaded laterally in cohesive soil", Géotechnique, 34, Issue 4, pp. 613-623.

Reul, O., Bauer, J., Mühl, A., Röder, K. (2013) "Messungen und numerische Untersuchungen zum Tragverhalten der Pfahlgründung für eine Brückenkrananlage im weichen Ton", Mitteilungen des Institutes und der Versuchsanstalt für Geotechnik der Technischen Universität Darmstadt, Heft 92, pp. 181 – 209.

Schenk, W., Smoltczyk, H-U. (1966) "Pfahlroste, Berechnung und Ausbildung", Grundbau-Taschenbuch, Abschnitt 2.7, Band 1, 2. Auflage, Ernst & Sohn Verlag, Berlin, pp. 658-715.

Schiffman, R. , L., Chen, A., T.-F., Jordan, J. (1969) "An Analysis of Consolidation Theory", Proc. ASCE, Journal of the Soil Mechanics and Foundations Division, SM1, Vol. 95, pp. 285-310.

Schultze, E., Muhs, H. (1967) "Bodenuntersuchungen für Ingenieurbauten", 2. Auflage, Springer Verlag,.

Stewart, D. P., Jewell, J. R., Randolph, M. F. (1994) "Design of piled bridge abutments on soft clay for loading from lateral soil movements", Geotechnique, 44, Issue 2, pp. 277-296.

Thá, P. C., Mühl, A., Glockner, A., Röder, K., Bazan, H. W. (2010) "Evaluation of the coefficient of earth pressure at rest K0 of a soft clay in Rio de Janeiro by using earth pressure cells, dilatometer tests and laboratory tests", Proc. XV COBRAMSEG, Gramado, Brazil, pp. 1-6.

Wenz, K.-P. (1963) "Über die Größe des Seitendrucks auf Pfähle in bindigen Erdstoffen" Institut für Boden- und Felsmechanik der Universität Karlsruhe, Heft 12.

Wenz, K.-P. (1972) "Seitendruck auf Pfähle in weichen bindigen Erdstoffen", Vorträge der Baugrundtagung 1972, Stuttgart, Deutsche Gesellschaft für Erd- und Grundbau, Essen, pp. 681-690.